UNIVERSITÀ DEGLI STUDI DI NAPOLI FEDERICO II

SCUOLA POLITECNICA E DELLE SCIENZE DI BASE

CORSO DI LAUREA IN INGEGNERIA AEROSPAZIALE

DIPARTIMENTO DI INGEGNERIA INDUSTRIALE

BACHELOR THESIS

PRELIMINARY SIZING AND FLIGHT PERFORMANCE OF A SINGLE-ELECTRIC POWERED RC AIRCRAFT

SUPERVISOR:
Dr.
CILIBERTI DANILO

CANDIDATE:
FRANCESCO GRANATA
Matricola: N35002616

CO-SUPERVISOR:
Prof. Eng.
NICOLOSI FABRIZIO

ANNO ACCADEMICO 2019/2020

AI MIEI GENITORI DEBORA E SERGIO E A NONNO GIOVANNI

CHE MI HANNO PERMESSO DI INSEGUIRE IL MIO SOGNO

PER ASPERA AD ASTRA!

Index

List of figures

List of tables

Chapter 1

Introduction

1. Team Organization

The team appointed to the realization of the model is a subgroup of the team formed in 2019 to participate in the Design Build and Fly (DBF) competition that would have been held the following year. The missions and requirements taken into consideration have been established starting from the ones of the competition. This project has given to each member of the team the opportunity to improve several soft skills such as team working and problem solving which are relevant and decisive for an engineer. In addition, this experience has allowed to deepen knowledge in the Aerospace Engineering field, providing the fundamentals of aircraft design in the context of an experimental bachelor's thesis.

The team counts five members to better focus each one's work on the five branches identified that will lead to the final design of the aircraft. Consequently, every member of the team is the leader of their own branch and therefore its manager. The team has been supervised by two advisors that proved guidance to the team throughout the whole project. The identified branches concern: the study of the aerodynamics of the aircraft through the use of software such as AIRFOIL and XFLR5; examination of the stability of the model with the aid of the program created by NASA, OpenVSP; structural analysis, in particular an accurate check was performed on the wing structure, in presence of aerodynamic loads; aircraft performance analysis (polar curves, propeller performance). It is clear that each branch is not isolated from the others, but there is a strong link between all the application fields considered and therefore a coordinated work by each member of the Team is required.

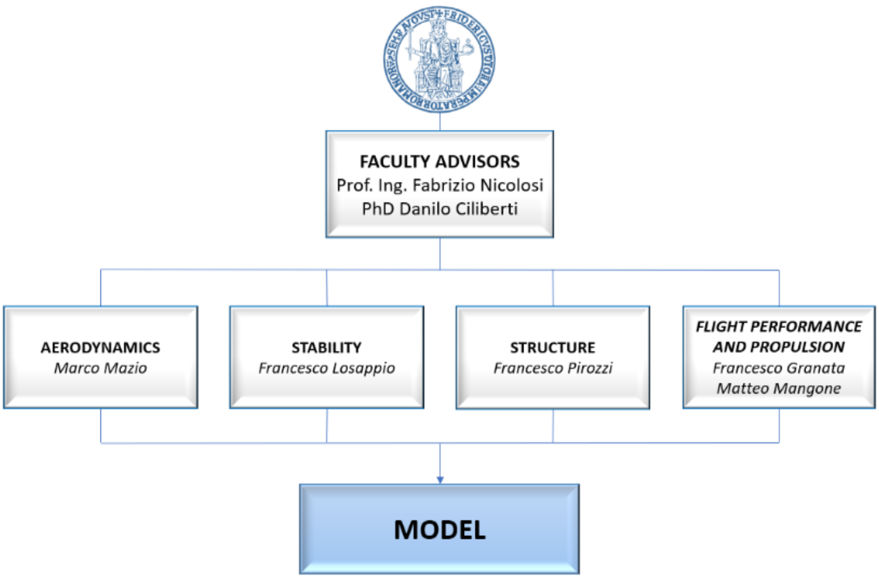

Figure 1 - Team Organization

1.1 Requirements

The main purpose of the team was to carry as many passengers as possible in order to allow the aircraft to conduct charter flights recovering expenses. In the table below, there is an overview of the requirements that the team had to respect during the project:

Maximum allowable wingspan	$5\ ft = 1{,}5\ m$
Take-Off Gross Weight with payload	$TOGW < 55\ lb = 25\ kg$
Passenger Weight	$5\ oz = 113{,}4\ g$
Luggage Weight	$1\ oz = 28{,}35\ g$
Take-Off Run	$23\ ft = 7\ m$
Ground for the take-off	$Dirt$
Endurance	$10\ min$
Minimum load for bending test	$\pm 3x\ MTOW$
Type of Propulsion	$Electric$

Table 1 - Requirements

In addition, the aircraft has to follow the path shown in the figure, and each lap must be completed in 2 minutes in order for passengers to have a comfortable and safe flight.

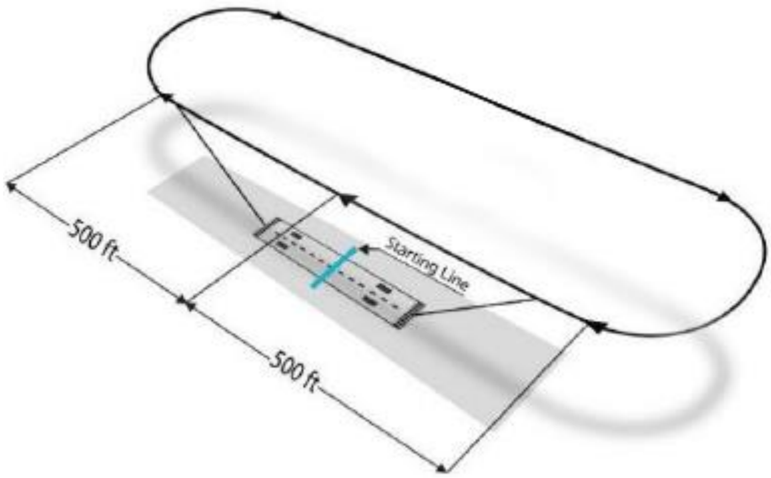

Figure 2 - AIAA Competition Flight Course

The dimension of each passenger and luggage are defined as it is showed below:

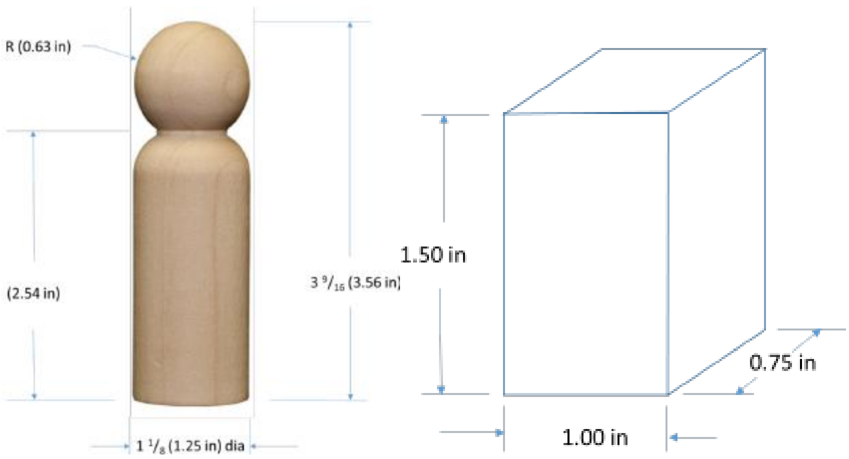

Figure 3 - Passenger and Luggage

Chapter 2

Preliminary Design and Sizing

2. Design Selection Process

In order to properly choose the best configuration for the aircraft, the team has compiled a table of merit based on the most important configuration factors. It has been assigned a score from 0 to 5 for each one, depending on the mission requirements.

Factor	Importance
Structural Weight	4
Maneuverability	3
Passengers Capability	5
Speed	3,5
Manufacturability	4,5
Take-OFF Run	2,5
Reliability	2,5

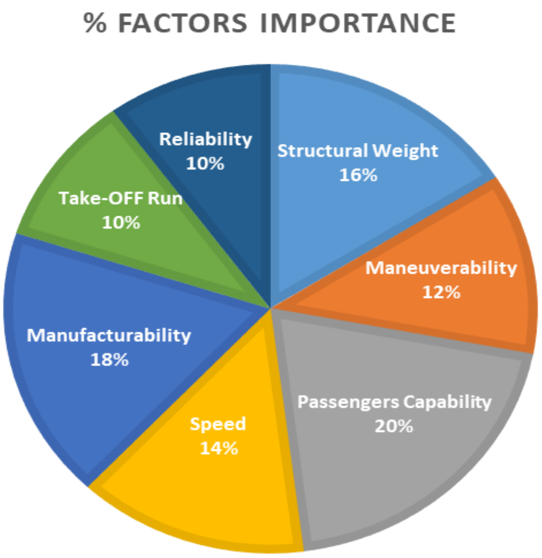

Table 2 - Table of merit

- **Structural Weight**: the weight strongly influences the performance of the aircraft, indeed a lower structural weight means whether less consumption or more payload transportable.
- **Maneuverability**: the capability to safely control the aircraft as well as its stability and fast maneuvers are also important to complete all the laps on time.
- **Passengers Capability**: this is the most important factor because carrying as many passengers as possible would provide more income for the charter company.
- **Speed**: the airplane speed contributes to complete faster the mission, although a trade-off study is necessary to avoid an excessive consumption of the batteries.

- **Manufacturability**: the ease of manufacturing is essential for building the aircraft by the team itself. Therefore, some configurations have been rejected due to tricky manufacturing and lack of solid executive experience alike.
- **Take-Off Run**: having a short take-off run is included among the requirements. This forced the team to take into account configurations that would provide advantages on those terms.
- **Reliability**: to guarantee the safety during the missions (take-off, cruise and landing), the reliablitiy of the aircraft is not a negligible factor.

Feature	Configuration	Wing	Tailplane	Engine	Landing Gear	Fuselage
Result	CONVENTIONAL	LOW	CONVENTIONAL	SINGLE/TWIN	TRICYCLE	RECTANGULAR

Table 3 - Final Design Decision

The final conceptual design has been chosen by analyzing the total score gained by each different configuration in terms of Structural Weight, Maneuverability, Passenger Capability, Speed, Manufacturability, Take-off Run and Reliability as shown so far. The total score is obtained by adding up scores assigned to each possible configuration as it will be shown further into this document.

2.1 Conceptual Design

Considering the requirements of the mission, it is appropriate to present the layout of the team’s arguments regarding how the bulk of the design was figured out. As a general note, the focus was on:

- Main wing configuration
- Main wing positioning
- Tail section
- Engines
- Landing gear
- Fuselage

This preliminary discussion is crucial in order to further analyse the capabilities of the aircraft. The choice made on those regards will form the foundations of the specialized studies that aim to reach the optimal configuration.

Component	**Alternatives**		
Wing Layout	Conventional	Biplane	Flying Wing
Wing Positioning	Low	High	
Empennage Type	V-Tail	Conventional	T-Tail
Number of Engines	1	2	
Landing Gear	Taildragger	Tricycle	
Fuselage section	Smoothed Rectangular	Circular	

Table 4 - Design Alternatives

2.1.1 Main Wing Configuration

The choice of the main wing configuration of the aircraft is the first aspect on which attention has been focused upon. That is because it is important to adapt the subsequent decisions regarding the individual components of the aircraft to this primary one.
The considered configurations are:

- CONVENTIONAL: it is composed by the tail plane (horizontal and vertical) and one main wing.
- BIPLANE: two overlapping wings which are parallel to each other although they may have different shapes and sizes.
- FLYING WING: flying wing aircraft without fuselage and tail plane.

By a structural weight's point of view, the best one is the flying wing since it is the lightest, because of the tail plane absence. However, the flying wing does not excel on directional stability due to the absence of the fin and this directly affects manoeuvrability. It is important to point out that the flying wing configuration will have a high longitudinal stability if equipped with reflex airfoil (self-stable) and if the warping factors and the sweep angle are well evaluated.

Regarding the biplane it must be said that with the same wingspan of a conventional configuration there is twice as much wing area, halving the wing load. Moreover, the eventual presence of a double aileron implies a higher roll rate and therefore more lateral manoeuvrability.

Focusing on reliability, the conventional configuration is the best known of the three considered and therefore well proven to be dependable. The biplane is frequently subject to assembly inaccuracies since it is the most complex.

Both the biplane and flying wing models are very difficult to manufacture because they require unconventional construction techniques. On the other hand, the conventional configuration is the simplest to manufacture.

The flying wing is the one that generates less drag among the three. On the other hand, the biplane configuration, with the presence of two main lift generators, create four vortex that massively increases aerodynamic drag. The conventional is a good compromise between the previous two.

Regarding the passenger's capacity, the biplane is the most inconvenient because it is difficult to create a passage for the insertion of passengers due to the presence of wing braces between the two wings.

Biplane configuration has a lower take off length since, with the same wingspan, the wing surface is two times bigger and therefore the wing load decreases. The opposite situation occurs with the flying wing, also because of the lack of flaps.

CONFIGURATION TRADE STUDY							
		CONVENTIONAL		FLYING WING		BIPLANE	
Attribute	Weighting	Insert Score	Weighted score	Insert Score	Weighted score	Insert Score	Weighted score
Structural Weight	16%	0.6	0.096	1	0.16	0.3	0.048
Manoeuvrability	12%	0.8	0.096	0.5	0.06	0.6	0.039
Passengers Capability	20%	0.8	0.16	0.3	0.06	0.7	0.081
Speed	14%	0.8	0.112	1	0.14	0.4	0.037
Manufacturability	18%	1	0.18	0.25	0.045	0.5	0.065
Take-Off Run	10%	0.9	0.09	0.7	0.07	1	0.083
Reliability	10%	1	0.1	0.5	0.05	0.6	0.055
Totals	100%		0.83		0.59		0.41

Table 5 - Configuration Trade Study

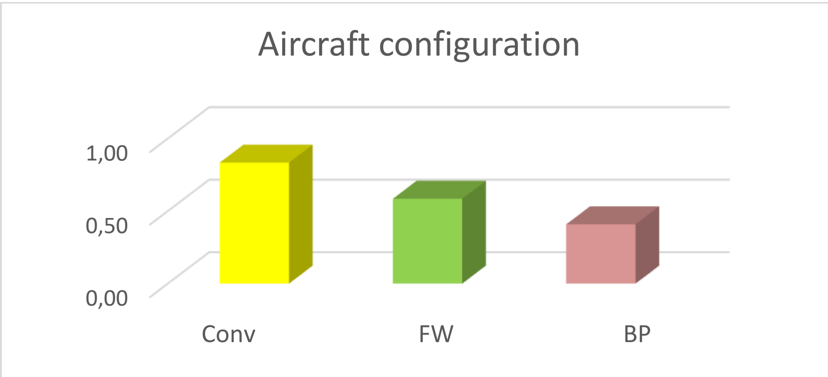

Figure 4 - Configuration Trade Study

2.1.2 Wing Positioning

Once opted for the conventional configuration for our aircraft, two different wing positions have been taken into consideration: high wing and low wing. As it is showed in the table below, the passenger capability is the parameter which most influenced our choice.

In terms of structural weight, the low wing configuration is slightly better because it allows to embed the spar in the force frames. This is not possible with a high wing that should be installed on the upper surface of the fuselage. However, in case of braced wing, the root sections could be slenderer because in that zone the momentum is null.

An aircraft with high wing has a better (static) lateral stability thanks to the dihedral effect (which gives a negative injection to the coefficient $C_{\mathcal{L}_\beta}$). Indeed, as shown in the figure below, a side wind (i.e. sideslip) causes an overpressure under the upwind wing and therefore the aircraft tends to stabilize thanks to the rolling moment generated. On the other hand, low wings provide better aerodynamic performance due to the absence of the joints between wing and fuselage, that is less interference drag. Moreover, it might help to reduce the take-off run taking advantage of the ground effect.

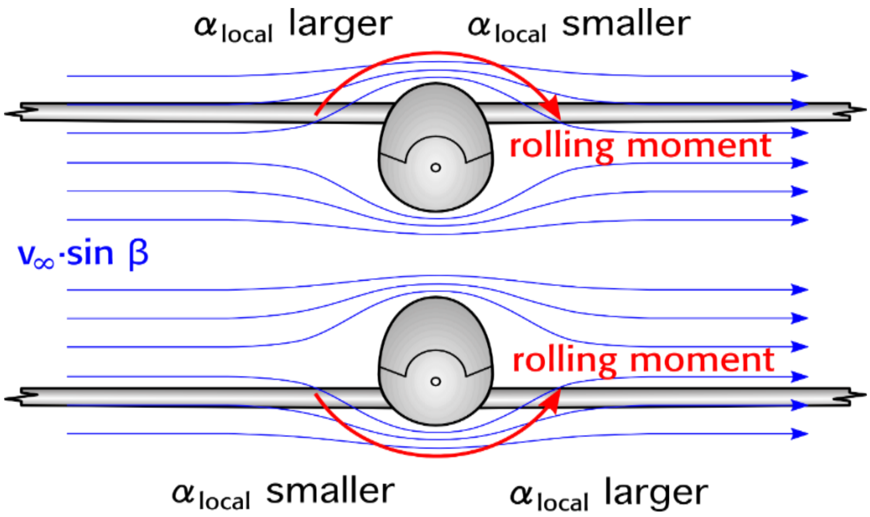

Figure 5 - Rolling Moment

As regards reliability, in case of imprecise landing, the high wing configuration is safer because the clearance is greater than it is with the low wing one which, instead, may impact on the ground if the airplane is banked.

The most important feature of the low wing configuration is that it guarantees a straightforward building and a simple access to the compartment where the passengers and luggage are stored. In addition, this configuration makes the assembly of the wing easier or its substitution alike. On the contrary, with a high wing, the loading and unloading of payload is likely to be trickier.

WING CONFIGURATION TRADE STUDY					
		HIGH		LOW	
Attribute	Weighting	Insert Score	Weighted score	Insert Score	Weighted score
Structural Weight	16%	0.4	0.064	1	0.16
Manoeuvrability	12%	0.6	0.072	0.8	0.096
Passengers Capability	20%	0.5	0.1	1	0.2
Speed	14%	0.4	0.056	0.7	0.098
Manufacturability	18%	0.6	0.108	0.9	0.162
Take-Off Run	10%	0.5	0.05	0.8	0.08
Reliability	10%	0.9	0.09	0.4	0.04
Totals	100%		0.54		0.836

Table 6 - Wing Configuration Trade Study

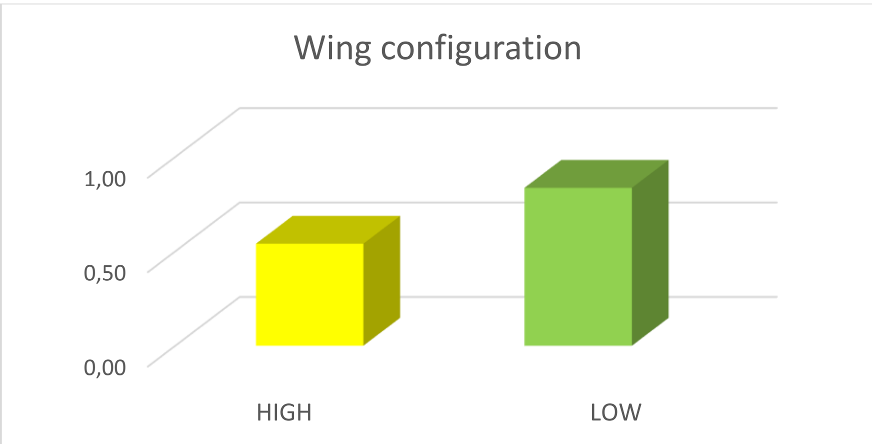

Figure 6 - Wing Configuration Trade Study

2.1.3 Tail

Once the configuration of the main wing is established, it is fundamental to discuss characteristics of the tail plane, specifically on a matter of stability, controllability, and reliability.

The main types of tail planes currently adopted by the aerospace industry are: conventional, T-tails, and V-tails. All of those options provide the aircraft with specific advantages and drawbacks that require a careful analysis.

It seems clear that the weight of the structure that support the aerodynamic surfaces of the tail plane will not be a major point of this discussion since it contributes only by a little percentage (estimated 5%) of the total inertial forces of the model aircraft.

The key point to analyse is instead how a different configuration plays into the overall stability and control of the aircraft, underlining the effect that each one has on the take-off distance.

The T-tail is composed by a vertical stabilizer which holds, within itself, the support structure of the horizontal stabilizer, placed at its tip. This particular kind of tail plane offers the advantage of working in an undisturbed airflow, allowing it to generate more lift at lower speed. Indeed, the dynamic pressure hitting the horizontal plane is unaffected by the downwash of the main wing, bringing the $\eta_H \cong 1$. At the same time, the horizontal tail reduces the magnitude of the vertical tail tip vortex, increasing the vertical tail effectiveness in sideslip, a phenomenon called end-plate effect.

Many times these advantages are outshined by a safety flaw of the T configuration. On extreme stall condition, the cone of turbulent flow coming from the main wing might engulf the tail plane, reducing its power of control turning it not effective altogether. This reason, along with an increased load on the vertical stabilizer, brought the team to reject the T-tail configuration.

T-tail is also prone to flutter, a dynamic aeroelastic phenomenon that must be avoided to fly safely. Tail flutter can rapidly destroy the empennage, leaving the aircraft without stability and control. To avoid flutter, the T-tail must have a very strong and rigid structure, which will increase the structural weight, opposing its aerodynamic advantage.

In contrast with all standard configurations, the V-tail consists in only two aerodynamic surfaces, they are tilted at an angle and often fixed on the upper side of the aircraft, effectively getting rid of one of the three wings that form the usual tail plane design. This of course makes the tail lighter, but, as we previously discussed, that is not an important issue for the analysis. Once again, the focus is on the ability of this configuration to provide stability and control authority during flight. The main feature of the V-tail is that the control power of rudder and equalizer is mixed and enforced using only two control surfaces. Yaw and pitch are consequently less effective unless the dimensions of the tail increase. This potential lack of power of the mixed equalizer might also result into a less performant take-off, that is one of the given requirements for the aircraft.

Therefore, the attention was focused on the conventional design for the tail plane. Both the deeper understanding for its properties and the possibility of installing a stabilator (since the stabilator is fitted into the fuselage) give this design an edge over the other two.

TAIL CONFIGURATION TRADE STUDY							
		T		Conventional		V	
Attribute	Weighting	Insert Score	Weighted score	Insert Score	Weighted score	Insert Score	Weighted score
Structural Weight	16%	0.7	0.112	1	0.16	0.5	0.08
Manoeuvrability	12%	1	0.120	1	0.120	0.2	0.024
Passengers Capability	20%	0	0.000	0	0.000	0	0.000
Speed	14%	0.8	0.112	1	0.140	1	0.140
Manufacturability	18%	0.75	0.135	1	0.180	0.1	0.018
Take-Off Run	10%	1	0.100	1	0.100	0.25	0.025
Reliability	10%	0.7	0.070	1	0.100	0.2	0.020
Totals	100%		0.65		0.80		0.31

Table 7 - Tail Configuration Trade Study

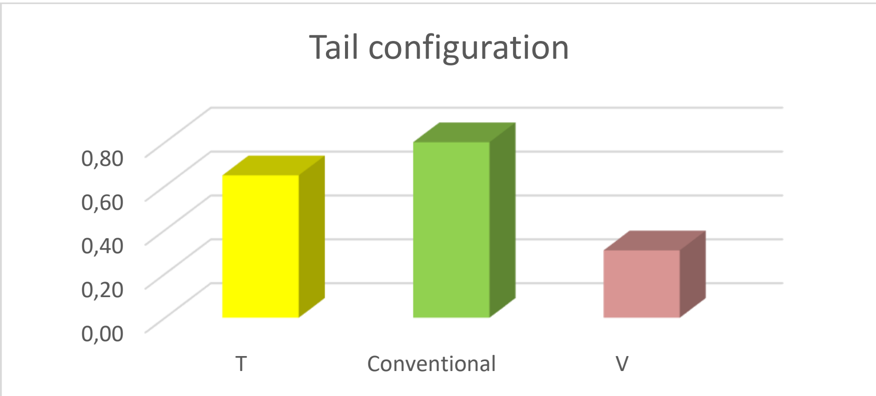

Figure 7 - Tail Configuration Trade Study

2.1.4 Number of Engines

Several factors were taken into account while conducting the propulsion system trade study for the aircraft. In particular, the aim of this section is to understand what the best number of engines is to install on the aircraft and therefore choose the single-engine configuration or the twin-engine configuration.

Firstly, a single engine configuration shall guarantee a certain overall weight saving since the battery pack should be lighter than the one needed for two engines. On the other hand, while a single engine would be installed on the aircraft's nose, in case of the twin-engine configuration, the engines would be installed on the wing structure. The presence of two inertial masses on the wing would make the total wing load decrease, thus the wing itself would be less stressed during flight. However, if the engines are installed on the wing, then a strengthened structure is needed where the engines are attached to the wing. That might mitigate the weight advantages aforementioned and would undermine the ease of manufacturing of the wing. Moreover, the CG of the wing sections that are behind the engine might shift ahead of the aerodynamic centre. This might increase the torque insisting on the wing structure.

The position of the engines also influences the manoeuvrability and stability of the aircraft. If the engine is on the aircraft's nose then it will not be influenced by the upwash generated by the wing, therefore the phenomena of non-axial flow, derived by the interaction air-wing, can be ignored. Furthermore, the energised flow behind the propeller increases the efficiency of the aerodynamic surfaces both of the horizontal tail plane and, in a lesser extent, the main wing. However, a twin-engine configuration ensures a better lateral control as it is possible to realise a differential thrust in order to help the rudder in case of need. At the same time, two engines require a bigger and strengthened rudder because it must guarantee directional controllability in case of one inoperative engine (OEI). It has to be said that in the unlucky event of a double engine failure, the presence of two propellers would induce more drag on the gliding aircraft than it would be if there was only one engine.

Moreover, two engines installed on the wing might be an obstacle while loading and unloading passengers as they would be close to the fuselage part that needs to be open during ground operations. Thus, for this reason and to guarantee a certain clearance from the ground, the propellers' diameter might need to be too limited. While it is true that in case of OEI condition a twin-engine configuration doesn't force the aircraft to abort the mission it is meant to accomplish, it also requires a more complicated electrical system and one more channel on the aircraft's controller than the single-engine configuration. Two engines also imply more maintenance and greater difficulty in case of substitution or repair of one of the engines.

In fact, it is not possible to decide without more specific considerations which configuration to choose. Therefore, once the aircraft geometry and structural characteristics will be more or less fixed, both studies about the single-engine and the twin-engine configuration will be further conducted to have a better understanding of the problem.

ENGINE CONFIGURATION TRADE STUDY					
	N	single		twin	
Attribute	Weighting	Insert Score	Weighted score	Insert Score	Weighted score
Structural Weight	16%	1	0.16	0.5	0.08
Manoeuvrability	12%	1	0.120	0.3	0.036
Passengers Capability	20%	0.6	0.120	1	0.200
Speed	14%	0.5	0.070	1	0.140
Manufacturability	18%	1	0.180	0.75	0.135
Take-Off Run	10%	0.7	0.070	1	0.100
Reliability	10%	0.5	0.050	1	0.100
Totals	100%		0.77		0.79

Table 8 - Engine Configuration Trade Study

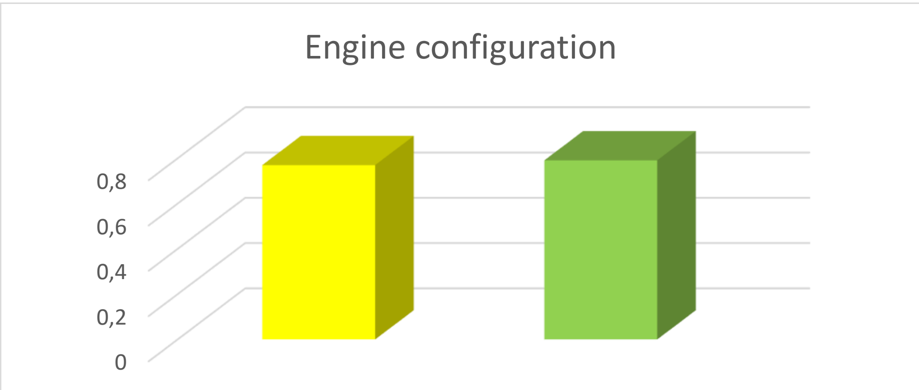

Figure 8 - Engine Configuration Trade Study

2.1.5 Landing Gear Type

Two different types of landing gear were compared. The first one is the tricycle landing gear that has a single nose wheel in the front, and two main wheels positioned close to the centre of gravity. The other alternative is the bicycle landing gear, also known as “taildragger”, which consists in a pair of wheels ahead the centre of gravity with an additional smaller wheel in the back of the plane.

By comparing the two solutions it was deduced that the tricycle leads to a greater structural weight than the bicycle. However, the weight gap is not wide enough to consider this aspect as a key factor for choosing one upon the other.

From the manoeuvrability point of view, it was found that the tailwheel-type landing gear, forces the aircraft to have a lower pitch angle during landing. That implies a strong use of the elevators to ensure a correct manoeuvre. Moreover, the relative position of CG and main landing gear does not mitigate the effect of the momentum generated by the friction between wheels and runway. Therefore, the rudder needs to make the aircraft stable also once it has touched the ground. On the other hand, the tricycle landing gear lets the aircraft fly at a greater angle of attack during approach to the runway, reducing landing speed and making the landing manoeuvre safer. The tricycle is also more stable during landing especially in case of single-engine configuration, as it guarantees more support to nose’s structure that carries the propeller and the engine.

The two-wheeled gear is aerodynamically convenient because the area exposed to the airflow is less than it is in the tricycle configuration.

The final boardable number of passengers will not be significantly affected by one of the different configurations considered. However, the tricycle is more comfortable because it does not involve any inclination of the fuselage during ground operations, so it is easier to load/unload passengers.

In case of the bicycle landing gear there is a greater inclination between the aircraft and the ground which implies a drag increment and it complicates the take-off manoeuvre. This condition stands until the aircraft is aligned with the runway. The bicycle landing gear is also preferable on grass airfield. On the other hand, the tricycle landing gear gives some advantages in terms of thrust during the take-off run because the thrust vector is parallel to the ground. That allows a greater acceleration to quickly reach lift-off speed. This alternative is most suitable for asphalted runways.

GEAR CONFIGURATION TRADE STUDY					
		BI		TRI	
Attribute	Weighting	Insert Score	Weighted score	Insert Score	Weighted score
Structural Weight	16%	1	0.16	0.8	0.128
Manoeuvrability	12%	0	0.000	0	0.000
Passengers Capability	20%	0	0.000	0	0.000
Speed	14%	1	0.140	0.95	0.133
Manufacturability	18%	0	0.000	0	0.000
Take-Off Run	10%	0.7	0.070	1	0.100
Reliability	10%	0.5	0.050	1	0.100
Totals	100%		0.42		0.46

Table 9 - Landing Gear Configuration Trade Study

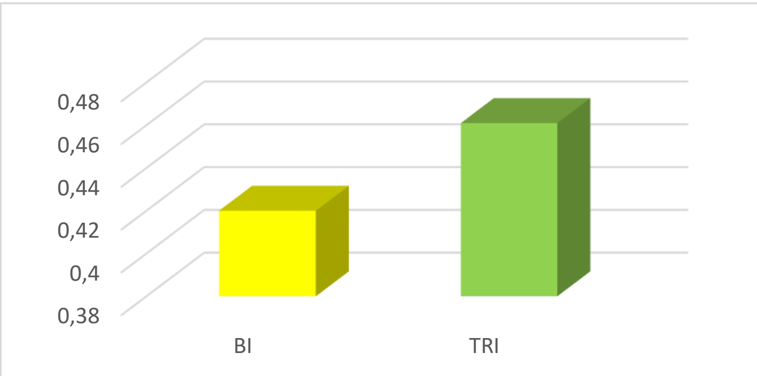

Figure 9 - Landing Gear Configuration Trade Study

2.1.6 Fuselage

The key factor for the analysis of the fuselage is the amount of payload it can carry. The types of fuselage taken into account are:

- CLASSIC: lobe structure which allows to define a practical shell structure involving curved plated beams and fuselage former.
- SMOOTHED RECTANGULAR: rectangular structure characterised by several corners that allow the structure itself to absorb greater loads. This phenomenon, however, means that in those points there is a greater probability of cracks propagation.

The smoothed rectangular section has a greater ease of construction and a better exploitability (more usable volume for a given section area) than the circular section.

FUSELAGE SECTION CONFIGURATION TRADE STUDY					
		SMOOTHED RECTANGULAR		CIRCULAR	
Attribute	Weighting	Insert Score	Weighted score	Insert Score	Weighted score
Structural Weight	16%	1	0.16	1	0.16
Manoeuvrability	12%	0	0.000	0	0.000
Passengers Capability	20%	1	0.200	0.75	0.150
Speed	14%	0.75	0.105	1	0.140
Manufacturability	18%	1	0.180	0.4	0.072
Take-Off Run	10%	0	0.000	0	0.000
Reliability	10%	1	0.100	0.75	0.075
Totals	100%		0.745		0.597

Table 10 - Fuselage Configuration Trade Study

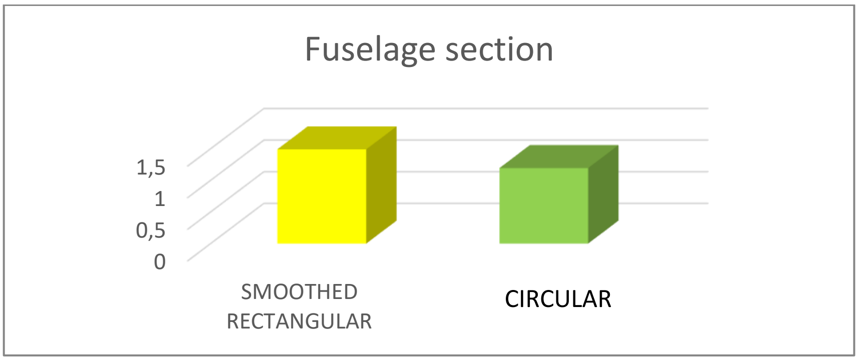

Table 11 - Fuselage Configuration Trade Study

2.2 Sizing Process

Estimating dimensions and weights of the aircraft is a crucial phase of the design process and it allows the team to develop more detailed analysis based on aerodynamics, structures, and flight performance. The sizing process consists in an iterative procedure which starts giving as input the wing load *W/S* (statistically set), a plausible take-off and landing lift coefficient and the distance of the take-off run according to the requirements. The process ends when the variation of the final weight assumes a value within the 3% compared to the previous iteration.

Before calculating the weights, the determination of the power loading $\frac{W}{\Pi}$, where W is the max take-off weight and Π is the engine max power, is essential. First of all, the stall speeds during landing and take-off are easily calculable knowing the density of the air, the wing load, and the two lift coefficients $C_{L_{max_L}}$ and $C_{L_{max_{TO}}}$.

After that, according to the constraint about the take-off distance, it is possible to establish the thrust-to-weight ratio by using the simplified formula of the take-off run as it follows:

$$S_G = \frac{1.21 \ W/S}{\rho g C_{L_{max_{TO}}} \ T/W} \quad \rightarrow \quad \frac{T}{W} = \frac{1.21 \ W/S}{\rho g C_{L_{max_{TO}}} S_G}$$

Since the aircraft is propeller-driven, the power instead of the thrust has been considered during calculations. A proper approximation in take-off conditions is:

$$T = \frac{\Pi \eta_p}{0.7 \cdot 1.21 V_{S_{TO}}}$$

Furthermore, assuming a propeller efficiency η_p value relatively low (between 0.5 and 0.6), the following relation has been considered:

$$\frac{\Pi}{W} = \frac{0.7 \cdot 1.21^2 \, W/S \, V_{S_{TO}}}{\eta_p \rho g C_{L_{max_{TO}}} S_G}$$

2.2.1 Weight Estimation

The characteristic weights of the aircraft are estimated in the following way.

The total weight (W) is given by the sum of different parts: structure, payload, engine (including prop), batteries, electronic parts. Passengers and their luggage constitute the payload to carry. They are respectively represented by standard cylinders and parallelepipeds made of wood. Their single weight is established by the requirements.

$$W = W_{\text{struct}} + W_{\text{payload}} + W_{\text{engine}} + W_{\text{batteries}} + W_{\text{electronic pts.}}$$

The structure's weight can be expressed by the following relation which takes into account the weight of the different structural components:

$$W_{\text{struct}} = W_{\text{wing}} + W_{\text{fuselage}} + W_{\text{h-tail}} + W_{\text{v-tail}} + W_{\text{gear}}$$

It is possible to statistically determine these weights by considering other aircraft with similar manufacturing characteristics (i.e. aircraft made of balsa wood). Then it is possible to evaluate for each component the weight to area ratio $W_{\text{comp}}/S_{\text{ref}}$ where S_{ref} is a characteristic surface of the component itself. That surface will be represented by the planform area for the wing and by the product of diameter and length for the fuselage (or eventually only for the length of the part with a constant cross section). The landing gear data can be obtained from statistics or relating it to the total weight. The $S_{\text{h-tail}}$ is considered as the 20-30% of the S_{wing}

$$\frac{W_{\text{wing}}}{S_{\text{wing}}} \quad \frac{W_{\text{fuselage}}}{D_{\text{fuselage}} L_{\text{fuselage}}} \quad \frac{W_{\text{h-tail}}}{S_{\text{h-tail}}} \quad \frac{W_{\text{v-tail}}}{S_{\text{v-tail}}} \quad \frac{W_{\text{gear}}}{S_{\text{gear}}} \quad \left(\text{or } \frac{W_{\text{gear}}}{W}\right)$$

The structure weight relation can be then developed by using these ratios as it follows:

$$W_{\text{struct}} = \frac{W_{\text{wing}}}{S_{\text{wing}}} S_{\text{wing}} + \frac{W_{\text{fuselage}}}{S_{\text{fuselage}}} S_{\text{fuselage}} + \frac{W_{\text{h-tail}}}{S_{\text{h-tail}}} S_{\text{h-tail}} + \frac{W_{\text{v-tail}}}{S_{\text{v-tail}}} S_{\text{v-tail}} + \frac{W_{\text{gear}}}{S_{\text{gear}}} S_{\text{gear}}$$

An iterative process is necessary as the surfaces considered before are initially unknown. Firstly, the areas values are assumed, then the weights of the single components are estimated as well as the total weight. Thus, the wing surface and the engine's weight can be determined by using the wing load and the power load previously obtained. The process explained is repeated until the difference between two consecutive iterations is less than 10 g.

It is assumed a wingspan of 5 ft by referring to the constraints given by the requirements and a value for the aspect ratio (i.e. AR = 8). It is also considered a rectangular wing because of its ease of manufacturing and its cost benefits:

$$AR = \frac{b^2}{S} \qquad S = \frac{b^2}{AR}$$

$$S = bc \qquad c = \frac{S}{b}$$

At this point it is necessary to check whether the chord's length obtained is realistic comparing it to the fuselage one. While length and diameter of the fuselage depend on the payload, the tail and nose lengths are statistically determined by considering the ones of similar aircraft.

As the structure weight is now known, the weight of electronic parts, engines and batteries needs to be defined. This is possible by using catalogues on the internet which associates the maximum power supplied by the engine to its weight and to recommended electronic parts, such as ESC and batteries. The following ratios can be then determined assuming an initial power of 300-600 W:

$$\frac{W_{engine}}{\Pi} \quad \frac{W_{\text{batteries}}}{\Pi} \quad \frac{W_{\text{electronic pts.}}}{\Pi}$$

	ITERATIONS									
			ITERATION N. 1		ITERATION N.2		ITERATION N.3		ITERATION N.4	
	Name	**Symbol**	**Quantity**	**Unit**	**Quantity**	**Unit**	**Quantity**	**Unit**	**Quantity**	**Unit**
	Power needed	Π_n	150.77	W	152.46	W	152.92	W	153.04	W
	ENGINE SYSTEM WEIGHT CALCULATION									
	Engine weight	W_{engine}	0.044	Kg	0.045	Kg	0.045	Kg	0.045	Kg
	Battery weight	W_{battery}	0.108	Kg	0.109	Kg	0.109	Kg	0.109	Kg
	ESC weight	W_{ESC}	0.016	Kg	0.016	Kg	0.016	Kg	0.016	Kg
	Engine Syst. weight	$W_{\text{engine.pts.}}$	0.168	Kg	0.170	Kg	0.171	Kg	0.171	Kg
	STRUCTURAL WEIGHT CALCULATION									
	Wing surface	S_{wing}	0.292	m^2	0.296	m^2	0.296	m^2	0.297	m^2
	Fuselage diameter	D_{fus}	0.130	m	0.130	m	0.130	m	0.130	m
	Fuselage length	L_{fus}	0.738	m	0.738	m	0.738	m	0.738	m
	Horizontal tail surface	$S_{\text{H\_tail}}$	0.058	m^2	0.059	m^2	0.059	m^2	0.059	m^2
	Vertical tail surface	$S_{\text{V\_tail}}$	0.020	m^2	0.021	m^2	0.021	m^2	0.021	m^2
	Structural weight estimate	W_{struct}	1.417	Kg	1.424	Kg	1.426	Kg	1.426	Kg
	Payload weight	W_{payload}	1.371	Kg	1.371	Kg	1.371	Kg	1.371	Kg
	Total aircraft weight	W_{tot}	2.956	Kg	2.965	Kg	2.967	Kg	2.968	Kg
CHECK	Chord	c	0.195	m	0.197	m	0.198	m	0.198	m
	Weight variation	ΔW	0.033	Kg	0.009	Kg	0.002	Kg	0.001	Kg

Table 12 - Iterations

LEGEND	
Input Data	
Iterations results	

PAYLOAD INPUT			
Name	**Symbol**	**Quantity**	**Unit**
Number of passengers	n	8	
Number of passengers for each row	N̲	2	
Passenger's length	a	0.031	m
Passenger's width	c	0.031	m
Passenger's height	l	0.09	m
Passenger's weight	M	113.4	g
Luggage length	a̲	0.019	m
Luggage width	c̲	0.025	m
Luggage height	l̲	0.038	m
Luggage weight	M̲	58	g

Table 13 - Payload Data Input

AIRCRAFT DATA INPUT			
Name	**Symbol**	**Quantity**	**Unit**
Wing Load	W/S	10 98	Kg/m^2 N/m^2
Maximum landing lift coefficient	$CL_{max\_landing}$	1.8	
Maximum take-off lift coefficient	$CL_{max\_takeoff}$	1.5	
Take-off run	S_g	7.0	m
Wingspan	b	1.5	m
Aspect Ratio	AR	8.0	

Table 11.2 – Aircraft Data Input

DESIGN			
Name	**Symbol**	**Quantity**	**Unit**
Stall speed - Landing	$V_{stall\_landing}$	3.0	m/s
Rate Thrust - Weight	T/W	0.0959	N/kg
Stall speed – Take-off	V_{stall_TO}	3.3	m/s
Rate Power-Weight	Π/W Π/W	5.257 51.57	W/N W/Kg
Structural Weight + Payload Weight	$W_{struct+payload}$	2.764	Kg
Structural Weight	W_{struct}	1.393	Kg
Payload Weight	$W_{payload}$	1.371	Kg
Power Required	Π_n	142.6	W
Electronics Weight	W_{elect}	0.159	Kg
Total Starting Weight	W_{tot}	2.923	Kg

Table 14 - Design Data

PAYLOAD STRUCTURE INFORMATION			
Name	**Symbol**	**Quantity**	**Unit**
Number of rows	N	4	
Passenger and Luggage seat length	a1	0.060	m
Passenger and luggage seat width	c1	0.037	m
Passenger and luggage height	H	0.108	m
Total length of payload grid	A	0.240	m
Total width of payload grid	C	0.074	m
Final length of payload grid	A_{final}	0.264	m
Final width of payload grid	C_{final}	0.081	m
Front part length	r	0.204	m
Tail length	j	0.270	m
Aircraft Length	L	0.738	m
Payload Weight	$W_{payload}$	1371.2	g

Table 15 - Payload Structure Information

STATISTIC ESTIMATION			
STRUCTURAL WEIGHT ESTIMATION			
RATIOS ESTIMATION			
Name	**Symbol**	**Quantity**	**Unit**
Wing's ratio	W_{wing}/S_{wing}	1.8300	Kg/m^2
Fuselage's ratio	$W_{fus}/(D_{fus} \cdot L_{fus})$	8.3000	Kg/m^2
Horizontal tailplane's ratio	W_{H_tail}/S_{H_tail}	1.0600	Kg/m^2
Vertical tailplane's ratio	W_{V_tail}/S_{V_tail}	1.2500	Kg/m^2
WEIGHTS ESTIMATION			
Name	**Symbol**	**Quantity**	**Unit**
Wing surface	S_{wing}	0.2813	m^2
Fuselage diameter	D_{fus}	0.1296	m
Fuselage length	L_{fus}	0.7383	m
Horizontal tailplane surface	S_{H_tail}	0.0563	m^2
Vertical tailplane surface	S_{V_tail}	0.0197	m^2
Structural Weight	W_{struct}	1.393	Kg

Table 16 - Weight Estimation

Considering the final values of weight regarding the electronics, the team selected real components that very closely match the ones coming from our model. The propulsion will be offered by the "A20-26 M EVO kv1130" by *Hacker* with the paired ESC "X-12-Pro". The battery that will power the propulsive system will be a "20C-ECO-X 1450mAh 3S-slim" from *TopFuel*.

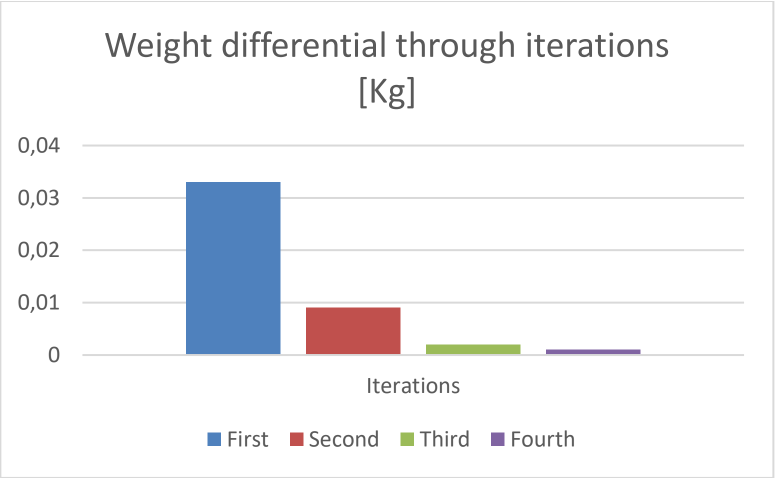

Figure 10 - Weight Differential through iterations

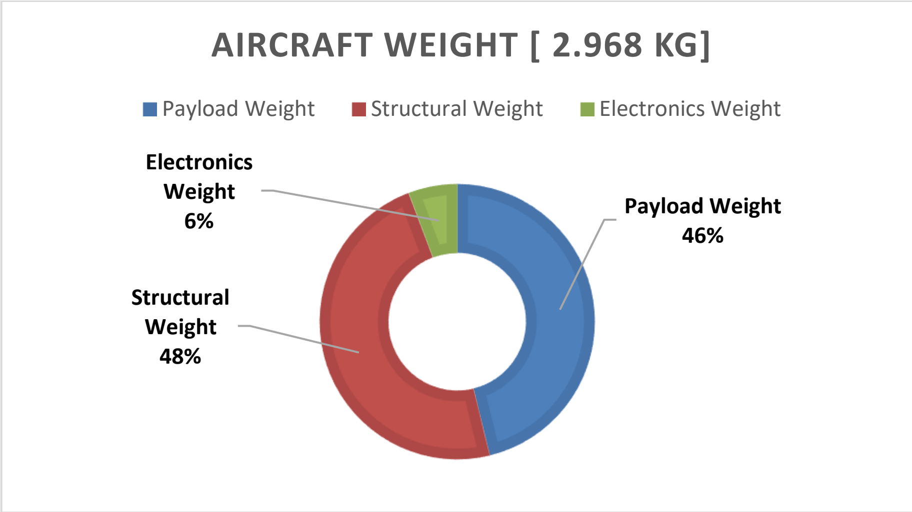

Figure 11 - Aircraft Weight

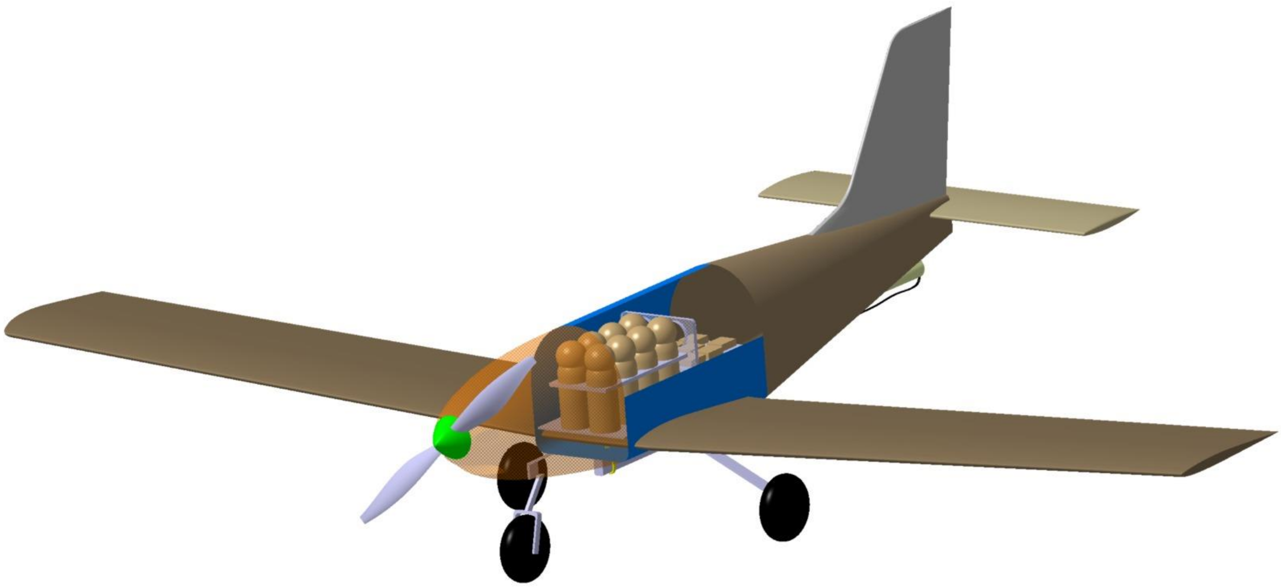

Figure 12 - First Aircraft Sketch

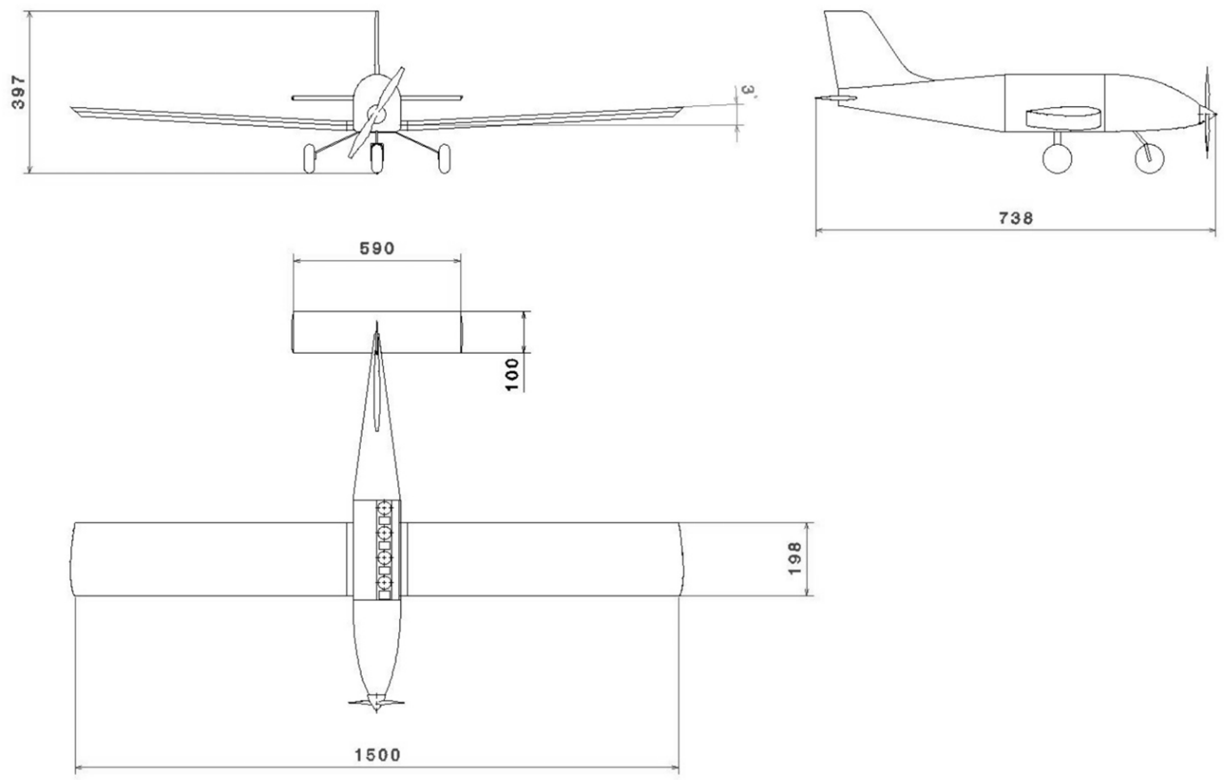

Figure 13 – Aircraft Three Views

Chapter 3

Flight Performance

3. Introduction

The aim of this section is to analyse the flight performance of the aircraft. In particular, calculations and theoretical considerations will be referred to the single engine configuration from now on.

The following performances were studied to ensure that the aircraft best meets the given requirements of the project:

- Take-Off
- Rate of Climb
- Maximum Cruise Speed
- Gliding Flight
- Turn
- Landing

3.1 Take-Off

The most important parameter related to the take-off is the take-off run because it is part of the given requirements for the aircraft. It is given by two contributes: ground run and airborne run.

Symbol	Quantity	Unit	Name
$C_{L\text{-}TO}$	1.5		Lift Coefficient during Take Off
n_{air}	1.2		Load Factor
μ	0.025		Friction Coefficient
W	2.92	Kg	Weight
$V_{st\text{-}TO}$	3.3	m/s	Stall Speed During Take Off
H	0.40	m	Obstacle height
φ	1		Throttle
η_p	0.7		Propeller Efficiency
Π_{a0}	157	W	Shaft Power
S	0.297	m^2	Wing Surface
$C_{D\text{-}TO}$	1		Drag Coefficient during Take Off

Table 17 - Take Off Input Data

The ground run is calculated considering the lift off speed as $V_{LO} = 1.1 \cdot V_{st-TO}$ and using the following approximated formula in which the total net force is considered a constant calculated at a speed of $0.7 \cdot V_{LO}$:

$$S_g = \frac{W}{2g} \cdot 1.21 \cdot \left(\frac{W}{S}\right) \cdot \left(\frac{2}{\rho}\right) \cdot \frac{1}{C_{L_{TO}}} \cdot \frac{1}{[T - D - \mu(W - L)]_{0.7\, V_{LO}}} = 4.48\, m$$

The take-off is considered finished when the aircraft flies over an imaginary obstacle whose height is reported in Table 17. Thus, it is necessary to determine the distance on the ground between that point and the lift off point as well as the radius and the angle of climb. They are respectively indicated as S_a, R and θ_{ob} as it follows:

$$R = \frac{(1.15 \cdot V_{st-TO})^2}{g \cdot (n_{air} - 1)} = 7.73\, m$$

$$\theta_{ob} = \arccos\left[1 - \frac{H}{R}\right] = 0.323 \text{ rad} = 18.52 \text{ deg}$$

$$S_a = R \cdot sin(\theta_{ob}) = 2.45\, m$$

Finally, it is possible to calculate the total take-off run:

$$S_{tot} = S_g + S_a = 6.93\, m$$

This is a very good result because it is compatible with the take-off run specified by the requirements (7 m long).

3.2 Climb

It is essential now to study the rate of climb (RC) of the aircraft and the related characteristic angles (θ).

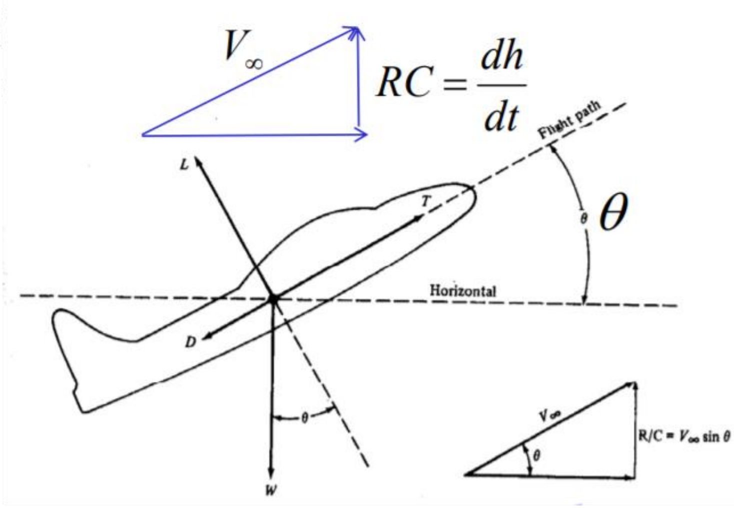

Figure 14 - Climb

In particular, the most important parameters are the maximum rate of climb and the angles (θ) related to the steepest climb and to the fastest climb. They are easily identifiable in the following speed versus RC diagram.

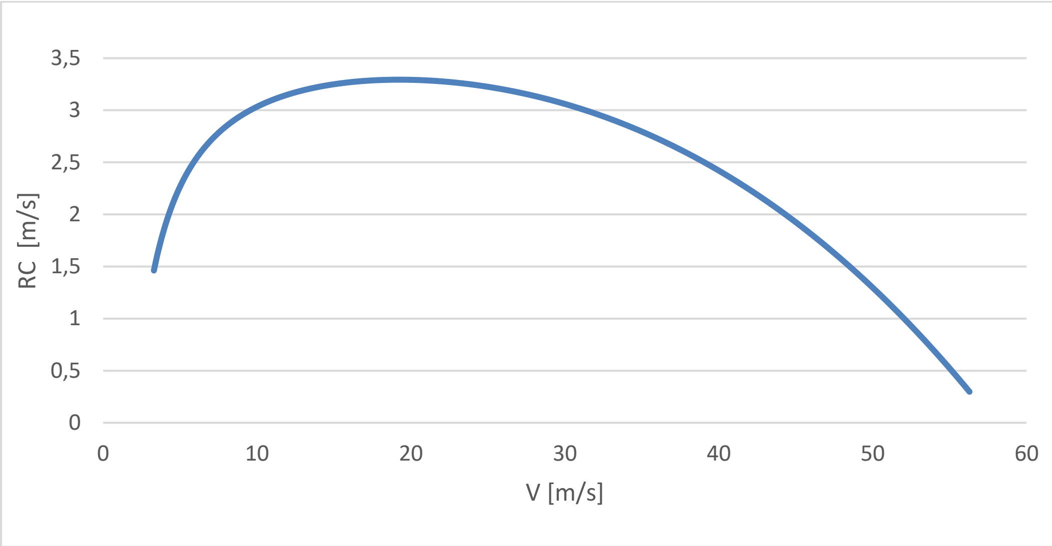

Figure 15 - Climb

Where the RC is related to the speed in this way:

$$RC = \eta_P \left(\frac{\Pi_{a,0}}{W}\right) - \frac{1}{2}\frac{\rho V^3 C_{D0}}{(W/S)} - \frac{2}{\pi AR_e}\frac{1}{\rho V}(W/S)$$

So, it results that: $RC_{max} = 3.29\, m/s = 11.84\, km/h$

The needed parameters aforementioned are obtained as it follows:

$$\theta = \arcsin\left[\frac{RC}{V}\right]$$

$\theta_{steep} = 27.99\, deg$

$\theta_{fast} = 9.82\, deg$

3.3 Turn

In a level turn the wing of the aircraft is tilted at an angle ϕ that is called bank angle. That implies a change in the direction of the lift and weight vectors.

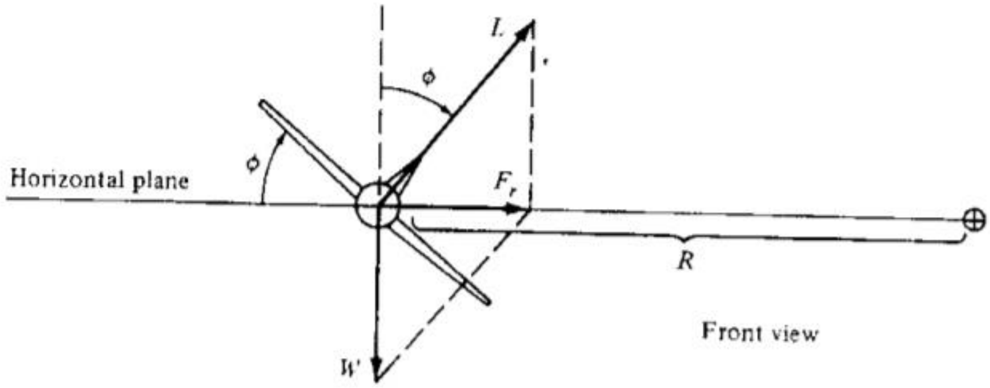

Figure 16 - Level Turn

The fundamental parameters to describe a level turn are the radius of turn *R*, the rate of turn ω and the load factor *n*.

$$R = \frac{V^2}{g \cdot \sqrt{n^2 - 1}} \qquad \omega = \frac{g \cdot \sqrt{n^2 - 1}}{V} \qquad n \stackrel{\text{def}}{=} \frac{L}{W} = \frac{1}{\cos\phi}$$

Considering a desired rate of turn *R* = 10 m, a cruise speed $V_{cruise} = 13$ m/s, a $C_{L\_max} = 1.3$ and a maximum load factor $n_{max} = 3.8$ the following values can be obtained:

$$n_{turn} = 1.99 \qquad \phi_{max} = \arccos\left[\frac{1}{n_{max}}\right] = 74.75\, deg$$

$$V_{st\_turn} = \sqrt{\frac{2 \cdot W \cdot n_{max}}{\rho \cdot s \cdot C_{L_{max}}}} = 6.85\ m/s = 24.66\, km/h$$

$$R_{min} = 1.30\, m \qquad \omega_{max} = 5.25\, rad/s$$

It is then necessary to verify that the power needed for a turn can be sustained by the aircraft engine:

$$\Pi_{no\_turn} = D \cdot V_{cruise} = 51.6\, W$$

Which is less than the available power so the aircraft can carry out the level turn.

3.4 Maximum Cruise Speed

The maximum cruise speed can be immediately obtained by considering the equilibrium equation $T = D$ and considering full throttle ($\phi = 1$).

$$V_{max} = 17.4\, m/s = 62.64\, km/h$$

3.5 Gliding Flight

Another crucial point is to understand the aircraft behaviour in the unlucky event of an engine failure that implies a gliding flight. Similarly to the climb, it is possible to plot the hodograph in which there is the rate of descent (RD) instead of the RC.

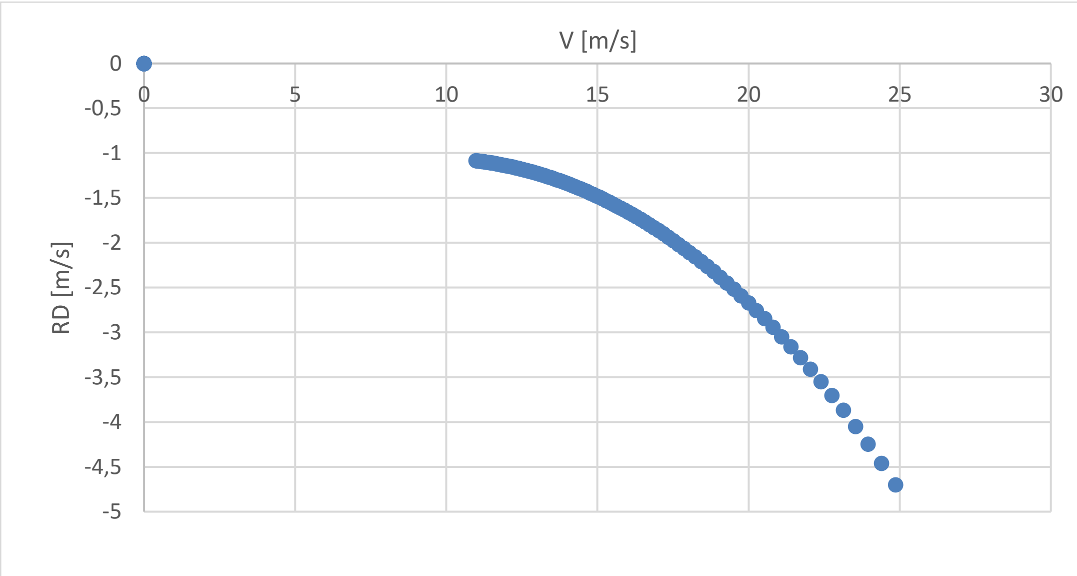

Figure 17 - Gliding Flight

The θ angle still is the angle between the flight path and the horizontal axis. It has to be said that the minimum angle possible is different from the one that guarantees the minimum RD. Indeed the θ_{min} is obtained when (C_L/C_D) is maximum (that means maximum efficiency) while the RD_{min} is obtained when $(C_L^{3/2}/C_D)$ is maximum. In this case:

$RD_{min} = -1.06\, m/s$ $\qquad$ $\theta_{min} = 5.41\, deg$

In general, the RD and θ are defined as it follows:

$RD = V \cdot \sin(\theta)$

$\theta = \arctan(1/E)$ where $E = C_L/C_D$ and its maximum value is $E = 10.57$

The maximum distance on the ground is obtained when RD is minimum, and it is:

$R_{max} = 717.67\, m$

considering that the gliding flight starts at an altitude $h = 50\, m$.

3.6 Landing

The landing performance was analysed supposing the following data:

Symbol	Quantity	Unit	Name
$C_{L\text{-landing}}$	1.8		Max Lift Coefficient during Landing
K_{ES}	0.9		Ground Effect Coefficient
μ	0.025		Friction Coefficient
W	2.92	Kg	Weight
$V_{st\text{-landing}}$	3.01	m/s	Stall Speed During Take Off
H	0.407	m	Approach Starting Height
$\varphi_{landing}$	0.05		Throttle
η_p	0.5		Propeller Efficiency
Π_{a0}	157	W	Shaft Power
S	0.297	m^2	Wing Surface
C_{D0}	0.045		Drag Coefficient

Table 18 - Landing Input Data

The landing manoeuvre can be divided into different stages: approach, flare, ground roll.

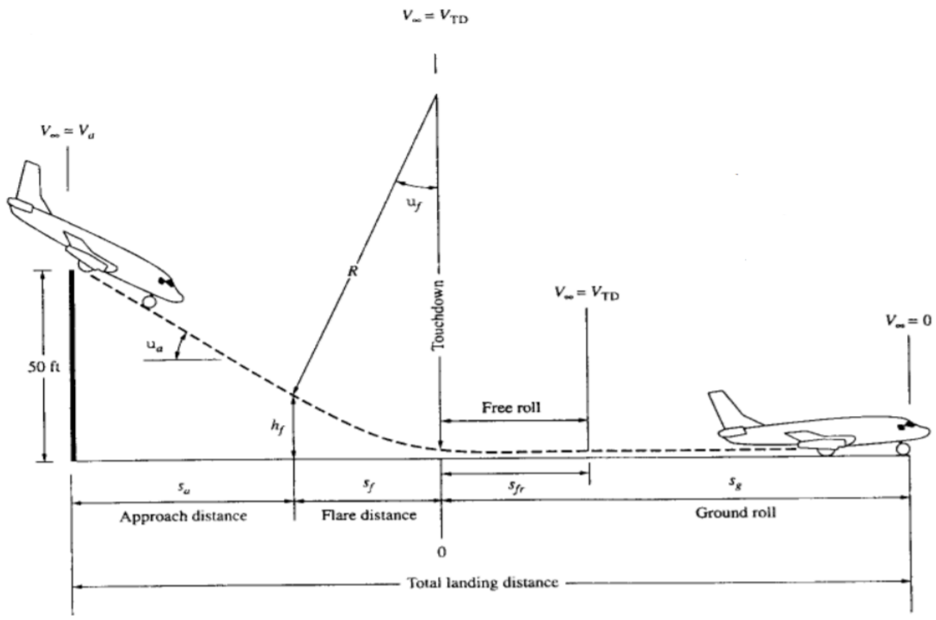

Figure 18 - Landing

The angle θ_a is necessary to determine the approach distance and it can be obtained in the following way:

$$\sin(\theta_a) = \frac{1}{E_a} - \frac{T_a}{W}$$

Where E_a is the efficiency during approach and T_a is the thrust during approach. They can be obtained considering:

$$V_a = 1.3 \cdot V_{st_{landing}} \qquad C_{L_a} = \frac{C_{L_{landing}}}{1.3^2} \qquad K_{Ta}(V) = 1 - 0.2\frac{V_a}{100}$$

$E_a = \frac{C_{L_a}}{C_{D_a}} = 8.14$ where $C_{D_a} = C_{D0} + \frac{{C_{L_a}}^2}{\pi \cdot AR_e} K_{es}$

$T_a = T_0 \cdot \varphi_{landing} \cdot K_{Ta}(V) = 1.49\ N$ where $T_0 = 30\ N$ is an input.

$\Rightarrow \quad \theta_a = 4.06\ deg$

The radius R can be calculated in the same way as it was in Sec. 3.1 considering a load factor n = 1.2 and a flare speed $V_f = 1.23 \cdot V_{st\_landing}$. Thus, the flare stage starts at the height h_f that can be found as it follows:

$R = 6.99\ m \ \Rightarrow \ h_f = R \cdot [1 - \cos(\theta_a)] = 0.018\ m$

From the previous input data the flare should start at about 2 cm from the ground. That is quite odd value if the airplane lands on grass. Therefore, it can be assumed a θ_a = 10 deg which leads to the following more realistic value:

$h_f = R \cdot [1 - \cos(\theta_a)] = 0.11\ m$

Finally, the approach distance can be found by solving the geometric problem:

$$S_a = \frac{H - h_f}{tan(\theta_a)} = 1.71\ m$$

Moreover, the flare distance can be immediately obtained in a similar way:

$S_f = R \cdot sin(\theta_a) = 1.21\ m$

The last contribute to the landing distance is given by the ground roll.

$$S_{gr} = \int_0^{V_{TD}} \frac{dV^2}{2 \cdot a}$$

It can be obtained approximating the acceleration as a constant equal to:

$$a_m = \frac{[D + \mu(W - L)]_{0.7\,V_{TD}}}{(W/g)} = 0.29\ m/s^2$$

Without wheel brakes the friction coefficient is as at take-off μ = 0.025:

$$S_{gr} = \frac{{V_{TD}}^2}{2 \cdot a_m} = 20.68\ m$$

Therefore, the total landing distance is:

$S_{tot} = S_a + S_f + S_{gr} = 23.6\ m$

3.7 Conclusion

The important results found in the previous sections are summed up in the following table:

Symbol	Quantity	Unit	Name
S_{tot-TO}	6.93	m	Take-Off Run
RC_{max}	3.29	m/s	Maximum Rate of Climb
V_{max}	62.64	km/h	Maximum Cruise Speed
RD_{min}	-1.06	m/s	Minimum Rate of Descent (Vertical Speed)
R_{max}	717.67	m	Maximum Gliding Distance
n_{turn}	1.99		Load Factor during a Level Turn
R_{min}	1.30	m	Minimum Radius of Turn
ω_{max}	5.25	rad/s	Maximum Rate of Turn
$S_{tot-landing}$	23.6	m	Landing Distance

Table 19 - Conclusions

Bibliography

[1] Lombardi, L., “ATR, Program review and market outlook”, 10th EWADE Conference, Naples, 2011.

[2] Special Convention RAA News. Regional horizons. RAA Annual Convention, Milwaukee, Wisconsin, May 2010.

[3] Bombardier Aerospace Commercial Aircraft Market Forecast. Commercial aircraft market forecast 2012-2031. 2012. URL: http://www2.bombardier.com/en/3_0/3_8/market_forecast.

[4] Simpson, R., Junction flows. Annual Review of Fluid Mechanics, 33, 2001.

[5] Hoerner, S. F., Fluid dynamic drag. Horner Fluid Dynamics, 1965.

[6] Schlichting, H., Truckenbrodt, E., A., “Aerodynamic of the Airplane,” 1st ed., McGraw-Hill, USA, 1979, Chaps 5, 6.

[7] Siegel, S., Comparison of design rules regarding the wing-body junction flow of a subsonic aircraft. University of Technology Dresden, Department of Aerodynamics, 30 June 2011.

[8] Jacobs E. and Ward, K., Interference of wing and fuselage from tests of 209 combinations in the NACA variable-density test tunnel. NACA Technical Report No. 540, 1935.

[9] Muttray,H., Aerodynamic aspects of wing-fuselage fillets. NACA Technical Memorandum No.764, 1935.

[10] Fleming, J., Simpson, R., Cowling, J. and Devenport, W., An experimental study of a turbulent wing-body junction and wake flow. Experiments in Fluids, 14, 1993.

[11] Oelcmen, S. and Simpson, R., Some structural features of a turbulent wing-body junction vortical flow. Report No. VPI-AOE-238, Virginia Polytechnic Institute and State University Blackburg, 1996.

[12] Boermans, L., M., M. and Nicolosi, F., “Sailplane fuselage and Wing-Fuselage junction design,” XXV Ostiv Congress, S. Auban France, 3-11 July 1997.

[13] Boermans, L. M. M., Nicolosi, F. and Kubrynski, K., Aerodynamic design of high performance sailplane wing fuselage combinations. 21st ICAS Conference, Paper No.A98-31523(ISBN-10:1-56347-287-2), 13 -18 September 1998.

[14] White, J. A. and Hood, M. J., Wing-fuselage interference tail buffeting and air flow about the tail of a low wing monoplatet, NACA Technical Report No.482, 1933.

[15] Maughmer,M., Hallmann,D., Ruszkowski, R., Chappel, G. and Waitz, I, Experimental investigations of wing-fuselage integration geometries, AIAA Journal of Aircraft, 26(8), 1989.